Published in final edited form as:
Int J Geriatr Psychiatry. 2012 October ; 27(10): 1017–1027. doi:10.1002/gps.2816.

Assessment of dementia risk in aging adults using both FDG-PET and FDDNP-PET imaging

L. M. Ercoli, **G. W Small**, **P. Siddarth**, **V. Kepe**, **S-C. Huang**, **K. J. Miller**, **H. Lavretsky**, **S. Y. Bookheimer**, **J. R. Barrio**, and **D. H. S. Silverman**
Department of Psychiatry and Biobehavioral Sciences and Semel Institute for Neuroscience and Human Behavior (L.M.E., P.S., K.J.M., J.K., S.Y.B., H.L., G.W.S.), Department of Molecular and Medical Pharmacology (D.H.S., V.K., S.-C.H., J.R.B.), Brain Mapping Center (S.Y.B.), Alzheimer's Disease Center (G.W.S., V.K.), and Center on Aging (G.W.S.), University of California, Los Angeles, Los Angeles, CA

Keywords

mild cognitive impairment; positron emission tomography; amyloid neuritic plaques; neurofibrillary tangles; glucose metabolism

Introduction

As therapeutic treatments for Alzheimer's disease (AD) are developed, the ability to identify persons prior to the clinical diagnosis of AD becomes increasingly important. Mild cognitive impairment (MCI) (Petersen et al., 1995, 2004) is a cognitive deficit syndrome associated with increased dementia risk. MCI is subtyped as amnestic or nonamnestic involving single or multiple cognitive domains (Winblad et al., 2003).

Amnestic MCI, particularly the multiple domain subtype, is associated with highest AD risk (Arnaiez et al., 2004; Bozoki et al., 2001; Petersen et al., 2009; Tabert et al., 2006) and progresses largely to AD at a rate of 10% to 15% annually (Farias et al., 2009). Autopsy studies show AD-like medial temporal neurofibrillary pathology as a predominate feature (Marksbury 2010; Petersen et al., 2006; Price and Morris et al., 1999).

Although amnestic subtypes have high AD risk, predicting AD from MCI subtypes is imprecise. Some patients remain stable, while others revert to normal cognition or develop non-AD dementias (e.g. vascular, frontotemporal) (Norbold et al., 2010; Petersen et al., 2004, Rozzini et al., 2007). Some amnestic MCI patients who progress to clinical AD do not demonstrate primary AD neuropathology (Jicah et al., 2008; Marksbury 2010).

The neuroimaging biomarker, 2-(1-{6-[(2-[F-18]fluoroethyl)(methyl)amino]-2-naphthylethylidene) malononitrile (FDDNP) labels senile plaques (SPs) and neurofibrillary tangles (NFTs) in vitro (Agdeppa et al., 2001). FDDNP-PET neuroimaging distinguishes

Address reprint requests to Linda Ercoli, Semel Institute, Rm 38-239, 760 Westwood Plaza, Los Angeles, CA, 90095-9668; phone (310) 825-9208; Fax (310) 267-0356; lercoli@mednet.ucla.edu.

among cognitively normal, MCI (predominately amnestic subtypes) and AD subjects (Small et al., 2006).DD Recently (Ercoli et al., 2009)D we hypothesized that if older adults vary according to cerebral patterns of SPs and NFTs, then FDDNP-PET imaging might identify homogeneous subgroups, which in turn may have implications for identifying individuals at highest AD risk. We then performed a cluster analysis according to regional FDDNP-PET binding values on a group combining subjects with either normal cognition or amnestic MCI (single or multiple domain subtypes). One FDDNP-subgroup (LG) had low FDDNP binding globally in all brain regions of interest (ROI), and two subgroups had relatively high FDDNP binding. One high binding subgroup demonstrated high frontal, parietal and medial temporal binding (HF/PA subgroup), and the other demonstrated high FDDNP binding in medial and lateral temporal and posterior cingulate regions (HT/PC subgroup). Notably, both the HF/PA and HT/PC subgroups showed similarly elevated medial temporal binding, but differed in binding levels in other ROI.

All three clusters included both MCI and cognitively normal subjects, but in different proportions. Most HT/PC and HF/PA subjects had amnestic MCI subtypes (71% for HF/PA; 88% for HT/PC) compared to 21% in LG. The HT/PC and HF/PA subgroups did not differ from each other on cognitive tests; however, both subgroups had worse performances relative to the LG subgroup in several domains. We would expect relatively lower AD risk in subjects with both low FDDNP binding and better cognition (i.e. LG subjects); and higher AD risk in subjects with both high FDDNP bin5ding and poor cognition (HT/PC and HF/PA subjects); however, additional supportive evidence of AD risk is needed.

The purpose of the current study was to further assess dementia risk associated with the FDDNP-subgroups by comparing them according to cerebral glucose metabolism with 2-deoxy-2-[F-18]fluoro-D-glucose (FDG) PET neuroimaging. FDG-PET has high sensitivity and specificity for autopsy confirmed AD and other neurodegenerative dementias (Silverman et al., 2001) D, and thus would provide external validation for dementia risk in the FDDNP-subgroups.

Methods

Subjects

The 54 subjects were from our previous report of differential FDDNP-PET binding patterns in non-demented subjects (Ercoli et al., 2009).X Subjects were volunteers recruited through advertisements and media coverage of a study of mild memory impairment, and referrals by physicians and families. The subjects were selected from an original volunteer pool of 116 persons who had undergone FDDNP scanning and cognitive testing as part of a large, ongoing study (Small et al., 2006). XXX We computed the FDDNP binding clusters using only the cognitively normal or amnestic MCI subtype subjects from the larger, ongoing study. We excluded 25 subjects with AD, 17 subjects with other diagnoses (e.g. frontotemporal dementia, depression), 5 subjects with non-amnestic MCI (because they are less likely to progress to AD), and 13 subjects who had head motion during scanning. Finally, two subjects from the previous study (Ercoli et al., 2009) who did not have FDG-PET scans suitable for spatial transformation to template space for quantitative assessments were not included. Investigators were unaware of the clinical data when excluding potential

subjects on the basis of PET scan quality and were unaware of the scans when excluding potential subjects on the basis of clinical data.

Of the 54 subjects, 10 with MCI were receiving cognitive enhancing drugs (a cholinesterase inhibitor or an N-methyl-D-aspartate receptor antagonist) at a steady dose for at least 3 months before study entry. All subjects underwent screening laboratory testing, neuropsychiatric evaluation, and structural imaging scanning to rule out other causes of cognitive impairment (e.g. stroke, brain tumor). Subjects with significant medical, neurological or psychiatric illness (e.g. major depression, psychotic disorders, seizures, head injury), diabetes (due to glucose injections for FDG-PET), cardiac abnormalities on EKG, uncontrolled hypertension, or MRI evidence of stroke or significant ischemia were excluded. Most subjects (N = 50) underwent magnetic resonance imaging (MRI). Four subjects who could not have MRIs had CT scans. All subjects received the Mini-Mental State Examination (Folstein, Folstein and McHugh, 1975), the Hamilton Rating Scale for Depression (Hamilton, 1960), a clinical interview, and a battery of neuropsychological tests (Lezak, Howieson and Loring, 2004).DD The test battery covered five cognitive domains: memory (Wechsler Memory Scale-Third Edition Logical Memory and Verbal Paired Associations II, Buschke-Fuld Selective Reminding Test, Rey-Osterrieth Complex Figure delayed recall); language (Boston Naming, F.A.S., Animal Naming tests); attention and speed of information processing (Trail Making Test-A, Stroop Color Naming [Kaplan version], and Wechsler Adult Intelligence Scale-Third Edition [WAIS-III] Digit Symbol); executive functioning (Trail Making Test-B, Stroop Interference, Wisconsin Card Sorting Test-Perseverative Errors); and, visuospatial functioning (WAIS-III Block Design, Rey-Osterrieth Complex Figure copy, Benton Visual Retention Test). Raw scores for cognitive tests in each domain were converted to Z scores and then averaged to form an average Z score for each domain (Bilder et al., 2000). Domain Z scores were the dependent variables for comparing clusters on cognitive tests.

Study clinicians (GWS, HL, KJM, LME) used clinical judgment (Petersen, 2004) and the following standard guidelines (Winblad et al., 2004) to diagnose MCI: (1) patient awareness of memory decline, preferably confirmed by another person; (2) greater-than-normal cognitive impairment on standardized tests; (3) normal daily activities performance, and (4) no dementia. The threshold for identifying mild impairment was scores ≥ 1 SD below age-corrected norms on neuropsychological tests for high sensitivity for predicting dementia (Busse et al., 2006; Jak et al., 2009). To balance increased sensitivity with specificity we required impairment on at least two neuropsychological tests per cognitive domain (Jak et al., 2009). Subjects with only memory impairment were diagnosed as single domain amnestic MCI (MCI-A); subjects with memory and other cognitive impairments were diagnosed with multiple domain amnestic MCI (MCI-A+); subjects with cognitively normal aging (CN) were without impairment. Functional abilities were assessed based on information obtained from the interview with corroboration by a collateral when possible.

Among MCI subjects, 13 had MCI-A and 15 had MCI-A+. The MCI subjects included 2 African-American, 1 Latino and 25 Caucasian individuals. The CN subjects included 1 African-American, 1 Latino and 24 Caucasians. Table 1 presents additional demographic data.

The study was conducted at UCLA. Written informed consent was obtained from all subjects in accordance with procedures of the Human Subjects Protection Committee of the University of California, Los Angeles and with the Helsinki Declaration of 1975, as revised in 1983. All subjects were able to provide consent. Cumulative radiation dosimetry for scans was below the mandated maximum annual dose and in compliance with state and federal regulations.

Scanning methods and analyses—All FDG-PET scans were performed with the ECAT HR or EXACT HR+ tomograph (Siemens-CTI, Knoxville, TN) with subjects supine with the imaging plane parallel to the orbito-meatal line. A bolus of FDG (370 MBq) was injected via an in-dwelling venous catheter and consecutive dynamic PET scans were performed for 60 mins. Scans were decay corrected and reconstructed using filtered back-projection (Hann filter, 5.5 mm FWHM) with scatter and measured attenuation correction. The resulting images contained 47 contiguous slices with plane separation of 3.37 mm (ECAT HR) or 63 contiguous slices with plane separation of 2.42 mm (EXACT HR+).

FDDNP preparation (Liu et al., 2007), FDDNP-PET acquisition and quantification of FDDNP binding are detailed elsewhere (Small et al., 2006). Briefly, quantification of FDDNP binding was performed with the Logan graphic method, with the cerebellum as the reference region (Logan et al., 1996; Kepe et al., 2006). The Relative Distribution Volume (DVR, the distribution volume of the tracer in an ROI divided by the distribution volume of the tracer in the reference) was obtained and DVR parametric images were generated. DVR images were analyzed using ROIs drawn manually on the co-registered MRI or CT scans for bilateral medial temporal (hippocampus, parahippocampal area and entorhinal cortex), lateral temporal, posterior cingulate, and frontal regions.

Anatomical MRI scans for 50 subjects were obtained using either a 1.5 Tesla (N = 16) or 3 Tesla (N = 34) magnet (General Electric-Signa, Milwaukee, WI) scanner. Fifty-four transverse planes were collected throughout the brain superior to the cerebellum using a double-echo, fast-spin echo series with a 24-cm field of view and 256 × 256 matrix with 3 mm/0 gap (TR = 6000 [3T] and 2000 [1.5T]; TE = 17/85 [3T] and 30/90 [1.5T]). Chi Square analyses indicated that frequency of subjects in the FDDNP-subgroups did not differ significantly according to MRI scanner [ChiSQ(2) = 1.03, p = .6].

Data analysis—Prior to statistical analyses, all data were inspected for outliers, skewness, kurtosis and homogeneity of variance to ensure appropriateness for parametric statistical tests.

Cluster Analysis: As previously described (Ercoli et al., 2009) XX, the FDDNP-PET subgroups resulted from a disjoint cluster analysis on the FDDNP binding (DVR) values for all subjects. The DVR values were first standardized to a mean of 0 and standard deviation of 1. Then, a disjoint cluster analysis was performed on the basis of Euclidean distances computed from the five regional FDDNP binding values (i.e. the k-means clustering method). Based on both the cubic clustering criterion and test statistics from the discriminant analyses, three clusters were identified as the optimal number—namely LG,

HT/PC and HF/PA. These FDDNP clusters served as independent variables for the following analyses:

Visual ratings of FDG-PET scans: All subjects were stratified into 7 groups (N1, N2, N3, P1, P1+, P2, P3) according to visual ratings of their cerebral metabolic pattern on the FDG-PET scans and relationships to autopsy-proven diagnostic categories (Silverman et al., 2001)XX. FDG-PET scan results were classified by a nuclear medicine physician blinded to all pathological and clinical information except age, sex, and (when available at the time PET had been performed) CT and MRI reports. PET scans were classified as indicative of a progressive or non-progressive clinical course. The metabolic patterns, detailed elsewhere (Silverman et al., 2001), are summarized as follows: normal (N1); normal except for age-appropriate atrophic changes (N2); abnormal only in a non-neurodegenerative pattern (N3); abnormal in a neurodegenerative pattern involving posterior cortical hypometabolism consistent with AD (P1); abnormal in a neurodegenerative pattern that includes posterior cortical hypometabolism but is nevertheless inconsistent with AD as the sole cause of dementia (P1+) (e.g., due to involvement of brain regions known to be preserved in AD); abnormal in a neurodegenerative pattern that is most consistent with frontotemporal dementia (P2), or a predominantly subcortical neurodegenerative process (P3). Figure 1 shows examples of visual ratings of FDG-PET scans. Inter-rater reproducibility between nuclear medicine physicians trained in visual categorization is high (94%, based upon blinded ratings of 100 FDG-PET scans) (Silverman et al., 2001). For statistical analyses, we applied chi-square tests to assess for associations involving the two broadest FDG diagnostic categories–between AD-like (P1, P1+) and non-AD-like (N1, N2, N3, P2, P3)—with FDDNP cluster assignments.

Standard statistical parametric mapping—FDDNP-subgroup-based differences in FDG scans were analyzed on a voxel-by-voxel basis using standard statistical parametric mapping techniques. As previously described, (Silverman et al., 2007) D images from all subjects were co-registered and reoriented into a standardized coordinate system using the SPM2 software package courteously provided by the image analysis team at the Wellcome Department of Cognitive Neurology, Functional Imaging Laboratory (London, UK). Data were then spatially smoothed and normalized to mean global activity. The set of pooled data were then assessed with the t- statistic on a voxel-by-voxel basis to identify the profile of voxels that significantly differed according to FDDNP-cluster subgroups. To protect against false positive findings potentially arising from multiple comparisons, results were considered significant only for uncorrected p values < 0.0005, and/or for voxels ≤ 0.001 located in the a priori regions corresponding to the specific patterns of FDDNP binding in the high-retention clusters (lateral temporal and posterior cingulate for HT/PC; frontal and parietal for HF/PA). Multiple comparison corrections made with family-wise error and/or false discovery rate adjustments at the voxel and cluster levels with $p < 0.05$ were also provided for each of the spm-based analyses.

Standardized region of interest (sROI) analysis—The sROI analyses were used to confirm and further detail the SPM mapping. FDG scans were quantified according to levels of activity present in a large panel of sROI's using computerized algorithms developed in

our group and subsequently implemented in the FDA-approved brain-PET software product NeuroQ(TM). The software measures, after correction for tissue-based attenuation, the number of radioactive events emitted by a positron source (gamma-ray lines of coincidence) per second detected by the PET scanner, emanating from pixel locations assigned by a computerized reconstruction algorithm as falling within each sROI. Mean pixel activity values were calculated within each of 240 sROI's defined throughout those transaxial planes across the field of view in which brain tissue was represented, following the transformation of each PET scan to a template space by a method previously described by Tai et al., (1997). The sROI's were then automatically grouped into 47 clusters of regions falling within structurally defined boundaries corresponding to distinct neuroanatomical (e.g. left inferior parietal lobule) or functional (e.g., Broca's area) standardized volumes of interest (sVOI's) and the mean activities for each of these volumes calculated. Finally, all mean activity values were automatically normalized to the mean pixel activity measured throughout that brain scan, or to the mean activity of an individual user-specified reference sVOI within that scan. Regional differences between FDDNP-cluster groups were assessed by Student's t or similar parametric tests.

Results

Subjects (Table 1) did not differ by age or education. MCI subjects had lower estimated premorbid IQ compared to CN subjects. More female subjects had MCI, but we did not control for gender because neither FDDNP binding nor resting state FDG-PET patterns of regional metabolism have been consistently found to significantly differ between men and women (Small et al., 2006; Volkow et al., 1997; Iseki et al., 2010; Hsieh et al., 2011). Table 2 shows cognitive status and test scores in the FDDNP clusters.

Visual FDG-PET scan ratings

The proportion of AD-like and non-AD-like FDG-PET patterns across the three FDDNP-subgroups differed significantly (exact chi-square ($df = 2$) = 6.98, $p < 0.03$) (Table 2). The HF/PA group had a predominantly AD-like FDG-PET pattern (14 of 24) while the LG and HT/PC groups had predominantly non-AD-like FDG-PET patterns (18 of 23 for LG; 5 of 7 for HT/PC). Thus, if a subject had an AD-like FDG-PET scan there was a 67% chance of being in the HF/PA FDDNP-subgroup and only a 33% chance of being in LG or HT/PC. By contrast, subjects with FDG-PET patterns inconsistent with increased AD risk had a 70% chance of being in the LG or HT/PC subgroups.

Within the Non-AD-like FDG group, most LG subjects were CN. Within the AD-like FDG group most HF/PA subjects were MCI, and most CN subjects were in LG. We found no significant differences in the distribution of MCI-A versus MCI-A+ subjects across the FDDNP-subgroups for either the AD-like or non-AD like FDG-PET group (Table 3).

SPM and region of interest analyses

Both analyses confirmed significant differences in the pattern of regional glucose metabolism among the FDDNP-subgroups. LG subjects had no areas of significant glucose hypometabolism relative to the other subgroups. HT/PC subjects had a preponderance of

hypometabolism in anterior temporal and frontal (i.e. left mid and inferior frontal gyrus interface area; anterior mid-temporal gyrus), posterior cingulate and bilateral parahippocampal regions (range, p.001 to < .0005) compared to LG (Figure 2). The sROI analysis confirmed that the most significant hypometabolism for HT/PC subjects occurred in anterior temporal cortex ($p<0.02$). The HT/PC subgroup showed relative hypermetabolism that was most significant in the superior parietal area (bilateral; right greater than left $p = .001$, also corroborated by sROI analyses) and anterior parietotemporal area ($p = .002$) compared to LG.

Subjects in HF/PA compared with those in LG demonstrated hypometabolism in bilateral inferior parietal/parietotemporal cortex (left more than right); bilateral posterior cingulate cortex; perisylvian regions; left mid temporal gyrus; and left dorsolateral prefrontal cortex (all having $p < .0005$) (Figure 3). The sROI analysis corroborated the most significant HF/PA hypometabolism occurring in left parietotemporal and posterior cingulate cortex ($p<0.01$). These patterns are consistent with increased AD risk.

Directly comparing the glucose metabolism of the HT/PC subgroup to the HF/PA subgroup, relative hypometabolism was found for HT/PC subjects in the left superior frontal gyrus, midbrain and hypothalamus. HF/PA subjects had lower glucose metabolism in bilateral inferior parietal regions compared to HT/PC subjects (range $p < .01$ to $< .001$).

Discussion

The current findings demonstrated that the three FDDNP-subgroups showed different glucose metabolic patterns from each other according to both visual ratings and SPM analyses of FDG-PET images. The FDG-PET scans of the lowest FDDNP binding (LG) subgroup were suggestive of relatively lower risk for AD. By contrast, the FDG-PET scans of subjects in the higher FDDNP binding subgroups (HT/PC and HF/PA) showed greater regional hypometabolism compared to LG and different glucose metabolic patterns from each other. The HF/PA group, with hypometabolism in mid-temporal, inferior parietal, posterior cingulate, and dorsolateral prefrontal regions, resembled a high AD risk pattern (Silverman et al., 2008). DLarge multi-center trials correlating FDG-PET imaging results with postmortem histopathological evaluation of brain tissue indicated that FDG-PET identified patients with autopsy confirmed AD with a sensitivity of 94% and specificity of 73%, and patients with neurodegenerative diseases of various kinds (e.g. frontotemporal dementia, Creutzfeld-Jacob disease, AD) with a sensitivity of 94% and a specificity of 78%.. (Silverman et al., 2001).

The meaning of the HT/PC FDDNP pattern is less clear. FDG-PET patterns for the HT/PC subgroup appeared neither normal nor AD-like. HT/PC may be an etiologically diverse group, including people with underlying cerebrovascular changes (Luchsinger et al., 2009; Marksbury et al., 2010; Petersen et al., 2006) or, with elevated frontotemporal dementia risk given the predominance of anterior frontal and anterior temporal hypometabolism (Foster et al., 2007; Silverman et al., 2001)

The current results are consistent with those of other studies that indicate the utility of combining neuroimaging approaches for early AD detection and for enhancing diagnostic

accuracy (Shin et al., 2010; Silverman et al., 2006). Using voxel based analyses, Shinn and colleagues (2010) compared FDG, FDDNP and PIB-PET images in the same subjects with either normal cognition or AD. SPM t maps of AD subjects' FDG-PET scans revealed hypometabolism in frontal, parietal, temporal and posterior cingulate/precuneus cortices. FDG hypometabolism and elevated FDDNP retention overlapped in the parietal region. FDG hypometabolism and high PIB retention overlapped in frontal, parietal, and temporal cortices. In the current study, the HF/PA FDDNP-PET pattern of relatively high frontal, parietal and medial temporal binding was most often associated with a high AD risk FDG-PET pattern. Taken together, the results support the combination of high amyloid and tau deposition and glucose hypometabolism in these regions as indicating high risk for AD.

The HF/PA subjects were also likely to demonstrate an AD risk FDG-PET pattern, which would be expected based on neuropathological determinations of the sequence of amyloid plaque and tau tangle brain accumulation in normal aging and MCI (Braak and Braak 1991, 1997; Petersen et al., 2006; Price and Morris, 1999). Patients with MCI already show predominate AD-like medial temporal tangle accumulation, which precedes the proliferation and spread of plaque and tangle deposition in frontal and parietal regions. Our finding that the HF/PA FDDNP-subgroup had AD-like FDG-PET patterns supports our prediction that the spread of these abnormal protein deposits to frontal and parietal regions indicates high risk for more accelerated neurodegeneration.

In this study, the amnestic MCI subtypes were similar with respect to FDG and FDDNP-PET patterns. Amnestic and non-amnestic MCI have been distinguished using FDG-PET in some studies (Clelisi et al., 2009; Jauhiainen et al., 2008) but not in others (Alexopoulos et al, 2009); and, no differences were found using PIB amyloid imaging (Wolk et al. 2009). The varied findings suggest that MCI reflects different cognitive manifestations of preclinical AD, several different underlying conditions, or a combination of both (Alexopoulos et al., 2009; Clerici et al., 2009). For instance, cerebrovascular risk and disease occur frequently in MCI subtypes and may play a role in progression to AD (Li et al., 2011; Luchsinger et al., 2009; van Straaten et al., 2008).

The current study has methodological limitations that could affect our results, their interpretation and generalizability, including partial volume effects (Protas et al., 2010)DD, error introduced from head motion during scanning (Wardas et al., 2010), relatively small subgroup sample, variability on outcomes due to MCI subtype heterogeneity, and the use of two different magnet strengths. Generalizability is limited to amnestic MCI subtypes.

The current findings provide external validation that different patterns of FDDNP-PET binding provides information about clinical prognosis as a result of independent validation from a well-established imaging method, FDG-PET. Moreover the HF/PA PET pattern was associated with greater AD risk according to FDG-PET scanning compared to the LG and HF/PA FDDNP patterns. Amnestic MCI subtypes had similar AD risk by neuroimaging standards. Longitudinal follow-up and the inclusion of other MCI subgroups and other diagnostic groups with amyloid or tau neuropathology are ongoing and will be important for further validating the current findings.

Conclusion

The FDDNP-subgroups demonstrated different glucose metabolic patterns according to both visual ratings and SPM analyses of FDG-PET data. FDG-PET provided independent validation that different patterns of FDDNP-PET binding in non-demented individuals may be associated with differential dementia risk.

Acknowledgments

Supported by NIH grants P01-AG024831, AG13308, P50 AG 16570, MH/AG58156, MH52453; AG10123; M01-RR00865, DOE contract DE-FC03-87-ER60615, GCRC Program, the Larry L. Hillblom Foundation, UCLA Semel Institute, California Department of Health and Human Services Alzheimer's Disease Project, Rotary CART Fund; Alzheimer's Association, UCLA Alzheimer's Disease Research Center (NIA/NIH AG16570); Turken Foundation, Fran and Ray Stark Foundation Fund for Alzheimer's Disease Research; Ahmanson Foundation; Lovelace Foundation, Judith Olenick Elgart Fund for Research on Brain Aging, the Brewster Foundation, and the Tamkin Foundation.

The authors thank Ms. Andrea Kaplan and Ms. Taylor Haight for help in subject recruitment, data management, and study coordination; Larry Pang and Hyong Oh for technical support, and Cheri Geist, Laura Pompano and Tiffany Chang for assistance with FDG-PET analysis' and N. Satyamurthy, Ph.D and the UCLA Biomedical Cyclotron staff for the synthesis of FDDNP.

The University of California, Los Angeles, owns the U.S. patent (6,274,119) entitled "Methods for Labeling β-Amyloid Plaques and Neurofibrillary Tangles," which has been licensed in the past to Siemens. Drs. Small and Barrio are among the inventors. Dr. Small reports having served as a consultant and received lecture fees from Eisai, Forest, Novartis, Pfizer, and Siemens. Dr. Lavretsky reports having received lecture fees from Eisai, Jannsen, and Pfizer and received a research grant from Forest. Dr. Barrio reports having served as a consultant and received lecture fees from Nihon Medi-Physics Co, Bristol-Meyer Squibb, PETNet Pharmaceuticals, and Siemens. Dr Barrio gratefully acknowledges the support of the Elizabeth and Thomas Plott Chair Endowment in Gerontology.

References

Agdeppa ED, Kepe V, Liu J, Flores-Torres S, et al. Binding characteristics of radiofluorinated 6-dialkylamino-2-naphthylethylidene derivatives as positron emission tomography imaging probes for beta-amyloid plaques in Alzheimer's disease. J Neurosci. 2001; 21(24):1–5.

Agdeppa ED, Kepe V, Liu J, et al. 2-Dialkylamino-6-acylmalononitrile substituted naphthalenes (DDNP analogs):novel diagnostic and therapeutic tools in Alzheimer's disease. Mol Imaging Biol. 2003; 5(6):404–17. [PubMed: 14667495]

Alexopoulos P, Grimmer T, Perneczky R, Domes G, Kurz A. Progression to dementia in clinical subtypes of mild cognitive impairment. Dement Geriatr Cogn Disord. 2006; 22(1):27–34. [PubMed: 16679762]

Arnáiz E, Almkvist O, Ivnik RJ, et al. Mild cognitive impairment: a cross-national comparison. J Neurol Neurosurg Psychiatry. 2004; 75(9):1275–80. [PubMed: 15314114]

Backman L, Jones S, Berger AK, Laukka EJ, Small BJ. Multiple cognitive deficits during the transition to Alzheimer's disease. J Intern Med. 2004; 256(3):195–204. [PubMed: 15324363]

Bilder RM, Goldman RS, Robinson D, et al. Neuropsychology of first-episode schizophrenia: initial characterization and clinical correlates. Am J Psychiatr. 2000; 7(4):549–59. [PubMed: 10739413]

Bozoki A, Giordani B, Heidebrink J, et al. Mild cognitive impairments predict dementia in nondemented elderly patients with memory loss. Arch Neurol. 2001; 58(3):411–6. [PubMed: 11255444]

Braak H, Braak E. Neuropathological staging of Alzheimer-related changes. Acta Neuropathol. 1991; 82(4):239–59. [PubMed: 1759558]

Braak H, Braak E. Frequency of stages of Alzheimer-related lesions in different age categories. Neurobiol Aging. 1997; 18(4):351–357. [PubMed: 9330961]

Busse A, Hensel A, Guhne U, et al. Mild cognitive impairment: long-term course of four clinical subtypes. Neurology. 2006; 67(12):2176–2185. [PubMed: 17190940]

Clerici F, Del Sole A, Chiti A, et al. Differences in hippocampal metabolism between amnestic and non-amnestic MCI subjects: automated FDG-PET image analysis. Q J Nucl Med Mol Imaging. 2009; 53(6):646–57. [PubMed: 20016455]

DeCarli C. Mild cognitive impairment: prevalence, prognosis, etiology, and treatment. Lancet Neurol. 2003; 2(1):15–21. [PubMed: 12849297]

Ercoli LM, Siddarth P, Kepe V, et al. Differential FDDNP PET patterns in non-demented middle-aged and older adults. Amer J Geriat Psychiatry. 2009; 17(5):397–406.

Farias ST, Mungas D, Reed BR, Harvey D, DeCarli C. Progression of mild cognitive impairment to dementia in clinic- vs community-based cohorts. Arch Neurol. 2009; 66(9):1151–7. [PubMed: 19752306]

Folstein M, Folstein S, McHugh P. "Mini-mental state": A practical method for grading the cognitive state of patients for the clinician. J Psychiatr Res. 1975; 12(3):189–98. [PubMed: 1202204]

Foster NL, Heidebrink JL, Clark CM, et al. FDG-PET improves accuracy in distinguishing frontotemporal dementia and Alzheimer's disease. Brain. 2007; 130(10):2616–35. [PubMed: 17704526]

Gorelick PB, Scuteri A, Black SE, Decarli C. Vascular Contributions to Cognitive Impairment and Dementia: A Statement for Healthcare Professionals From the American Heart Association/ American Stroke Association. Stroke. 2011 Jul 21. [Epub ahead of print].

Hamilton M. A rating scale for depression. J Neurol Neurosurg Psychiatry. 1960; 23:56–62. [PubMed: 14399272]

Hsieh TC, Lin WY, Ding HJ, et al. Sex- and Age-Related Differences in Brain FDG Metabolism of Healthy Adults: An SPM Analysis. J Neuroimaging. 2011 Feb 18. [Epub ahead of print]. 10.1111/j.1552-6569.2010.00543.x

Iseki E, Murayama N, Yamamoto R, et al. Construction of a (18)F-FDG PET normative database of Japanese healthy elderly subjects and its application to demented and mild cognitive impairment patients. Int J Geriatr Psychiatry. 2010; 25(4):352–61. [PubMed: 19693778]

Jak AJ, Bondi MW, Delano-Wood L, et al. Quantification of five neuropsychological approaches to defining mild cognitive impairment. Am J Geriatr Psychiatry. 2009; 17(5):368–75. [PubMed: 19390294]

Jauhiainen AM, Kangasmaa T, Rusanen M, et al. 8Differential hypometabolism patterns according to mild cognitive impairment subtypes. Dement Geriatr Cogn Disord. 2008; 26(6):490–8. [PubMed: 18987469]

Jicha GA, Parisi JE, Dickson DW, et al. Neuropathologic outcome of mild cognitive impairment following progression to clinical dementia. Arch Neurol. 2008; 63(5):674–81. [PubMed: 16682537]

Kepe V, Huang SC, Small GW, Satyamurthy N, Barrio JR. Visualizing pathology deposits in the living brain of patients with Alzheimer's disease. Methods Enzymol. 2006; 412:144–60. [PubMed: 17046657]

Lezak, M.; Howieson, D.; Loring, D. Neuropsychological assessment. 4. New York: University Press; 2004.

Li J, Wang YJ, Zhang M, et al. Vascular risk factors promote conversion from mild cognitive impairment to Alzheimer disease. Neurology. 2011; 76(17):1485–91. [PubMed: 21490316]

Liu J, Kepe V, Žabjek A, et al. High Yield, Automated Radiosynthesis of 2-(1-{6-[(2-[18F]Fluoro-ethyl)(methyl)amino]-2-naphthyl}ethylidene)malononitrile ([18F]FDDNP). Ready for Animal or Human Administration. Mol Imaging Biol. 2007; 9(1):6–16. [PubMed: 17051324]

Logan J, Fowler JS, Volkow ND, et al. Distribution volume ratios without blood sampling from graphical analysis of PET data. J Cereb Blood Flow Metab. 1996; 16(5):834–40. [PubMed: 8784228]

Luchsinger JA, Brickman AM, Reitz C, et al. Subclinical cerebrovascular disease in mild cognitive impairment. Neurology. 2009; 73(6):450–6. [PubMed: 19667320]

Markesbery WR. Neuropathologic alterations in mild cognitive impairment: a review. J Alzheimers Dis. 2010; 19(1):221–8. [PubMed: 20061641]

Nordlund A, Rolstad S, Klang O, et al. Two-year outcome of MCI subtypes and aetiologies in the Göteborg MCI study. J Neurol Neurosurg Psychiatry. 2010; 81(5):541–6. [PubMed: 19965857]

Petersen RC, Smith GE, Ivnik RJ, et al. Apolipoprotein E status as a predictor of the development of Alzheimer's disease in memory-impaired individuals. JAMA. 1995; 273(16):1274–8. [PubMed: 7646655]

Petersen RC. Mild cognitive impairment as a diagnostic entity. J Intern Med. 2004; 256(3):183–94. [PubMed: 15324362]

Petersen RC, Parisi JE, Dickson DW, et al. Neuropathologic features of amnestic mild cognitive impairment. Arch Neurol. 2006; 63(5):665–72. [PubMed: 16682536]

Petersen RC, Roberts RO, Knopman DS, et al. Mild cognitive impairment: ten years later. Arch Neurol. 2009; 66(12):1447–55. [PubMed: 20008648]

Protas HD, Huang S-C, Kepe V, Hayashi K, Klunder A, Braskie MN, et al. FDDNP binding using MR derived cortical surface maps. Neuroimage. 2010; 49:240–48. [PubMed: 19703569]

Price JL, Morris JC. Tangles and plaques in nondemented aging and "preclinical" Alzheimer's disease. Ann Neurol. 1999; 45(1):358–368. [PubMed: 10072051]

Rozzini L, Chilovi BV, Conti M, et al. Conversion of amnestic Mild Cognitive Impairment to dementia of Alzheimer type is independent to memory deterioration. Int J Geriatr Psychiatry. 2007; 22(12):1217–22. [PubMed: 17562522]

Silverman DH, Small GW, Chang CY, et al. Positron emission tomography in evaluation of dementia: Regional brain metabolism and long-term outcome. JAMA. 2001; 286(17):2120–7. [PubMed: 11694153]

Silverman DH, Cummings JL, Small GW, et al. Added clinical benefit of incorporating 2-deoxy-2-[18F]fluoro-D-glucose with positron emission tomography into the clinical evaluation of patients with cognitive impairment. Mol Imaging Biol. 2002; 4(4):283–93. [PubMed: 14537119]

Silverman DH, Dy CJ, Castellon SA, et al. Altered frontocortical, cerebellar, and basal ganglia activity in adjuvant-treated breast cancer survivors 5–10 years after chemotherapy. Breast Cancer Res Treat. 2007; 103(3):303–11. [PubMed: 17009108]

Silverman DH, Mosconi L, Ercoli L, Chen W, Small GW. Positron emission tomography scans obtained for the evaluation of cognitive dysfunction. Semin Nucl Med. 2008; 38(4):251–61. [PubMed: 18514081]

Small GW, Kepe V, Ercoli LM, et al. PET of brain amyloid and tau in mild cognitive impairment. N Engl J Med. 2006; 355(25):2652–63. [PubMed: 17182990]

Tabert MH, Manly JJ, Liu X, Pelton GH, et al. Neuropsychological prediction of conversion to Alzheimer disease in patients with mild cognitive impairment. Arch Gen Psychiatry. 2006; 63(8): 916–24. [PubMed: 16894068]

Tai YC, Lin KP, Hoh CH, Huang SC, Hoffman EJ. Utilization of 3-D elastic transformation in the registration of chest X-ray CT and whole body PET. IEEE Trans Nucl Sci. 1997; 44(4):1606–1612.

Troncoso JC, Martin LJ, Dal Forno G, Kawas CH. Neuropathology in controls and demented subjects from the Baltimore Longitudinal Study of Aging. Neurobiol Aging. 1996; 17(3):365–371. [PubMed: 8725897]

van Straaten EC, Harvey D, Scheltens P, et al. Periventricular white matter hyperintensities increase the likelihood of progression from amnestic mild cognitive impairment to dementia. J Neurol. 2008; 255(9):1302–8. [PubMed: 18825439]

Volkow ND, Wang GJ, Fowler JS, et al. Gender differences in cerebellar metabolism: test-retest reproducibility. Am J Psychiatry. 1997; 154(1):119–21. [PubMed: 8988972]

Wardak M, Wong KP, Shao W, et al. Movement correction for improving quantitative analysis of dynamic brain 18F-FDDNP PET. J Nucl Med. 2010; 51(2):210–18. [PubMed: 20080894]

Winblad B, Palmer K, Kivipelto M, et al. Mild cognitive impairment—beyond controversies, towards a consensus: report of the International Working Group on Mild Cognitive Impairment. J Intern Med. 2004; 256(3):240–46. [PubMed: 15324367]

Wolk DA, Price JC, Saxton JA, et al. Amyloid imaging in mild cognitive impairment subtypes. Ann Neuro. 2009; 65(5):557–68.

Key Poins

1. Positron emission tomography with 2-(1-{6-[(2-[F-18]fluoroethyl)(methyl) amino]-2-naphthyl} ethylidene)malononitrile (FDDNP), a molecule that binds to plaques and tangles in vitro, identified three subgroups of non-demented subjects according to FDDNP binding patterns: (a) relatively low FDDNP binding throughout the brain (LG); (b) high medial, lateral temporal and posterior cingulate binding (HF/PA); and (c) high frontal, parietal and medial temporal binding (HT/PC).
2. FDG-PET provided independent validation that different patterns of FDDNP-PET binding in non-demented individuals may be associated with differential dementia risk.
3. The FDG-PET pattern for the HF/PA FDDNP subgroup was consistent with increased AD risk. The FDG-PET pattern for the HT/PC FDDNP subgroup suggested a heterogeneous etiological group. The FDG-PET pattern for the LG FDDNP subgroup showed relatively no hypometabolism, and was consistent with lowest risk for AD.

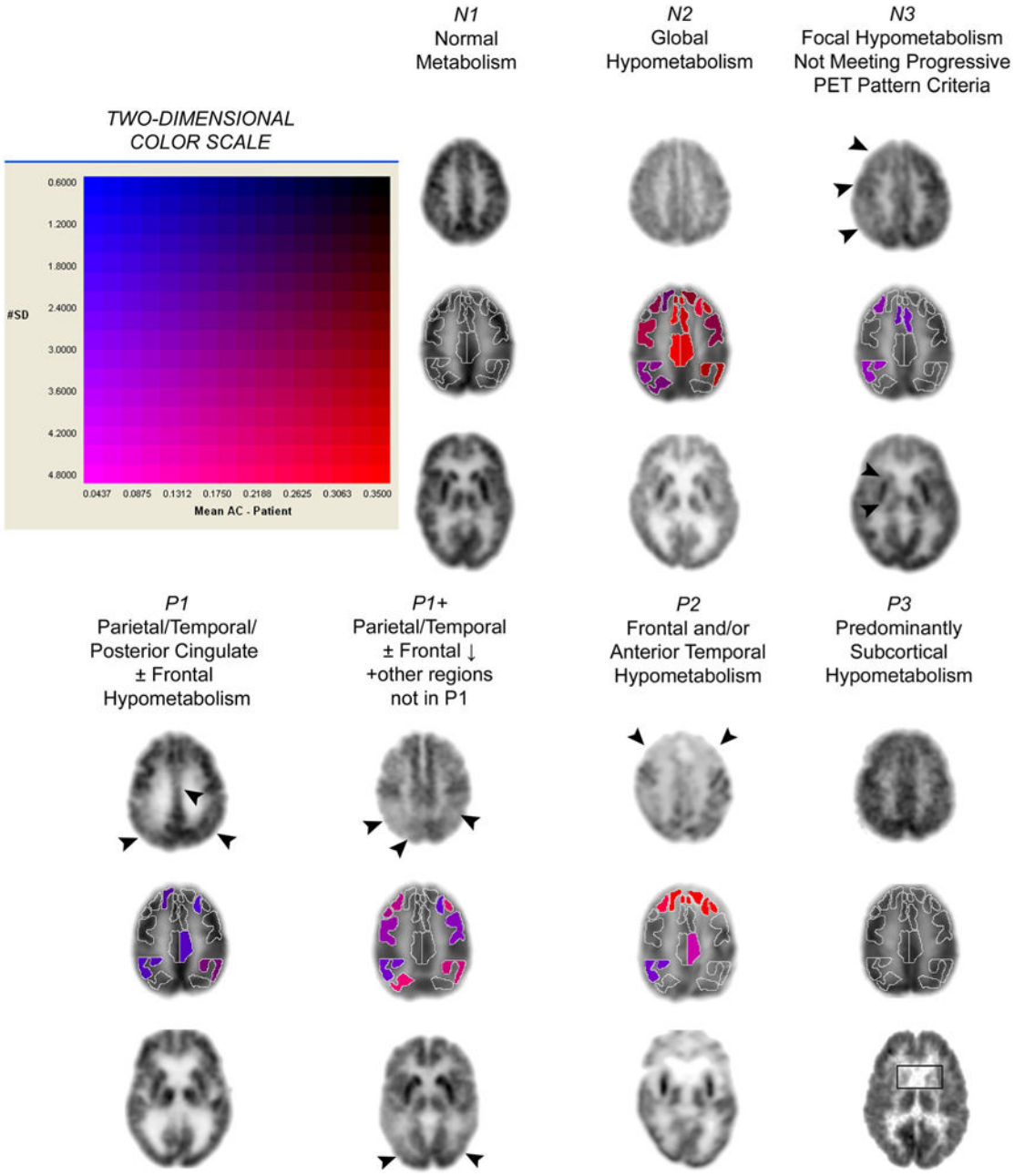

Figure 1.

Typical patterns of FDG distribution in brains of subjects undergoing evaluation for cognitive dysfunction. For the seven columns of images, each representing a distinct pattern of regional cerebral glucose metabolism (N1, N2, N3, P1, P1+, P2, and P3, as described in the text), the top row depicts a high transaxial slice (at the level of cingulate cortex), the bottom row depicts a mid-transaxial slice (at the deep gray matter level) from the same subject, and the middle row shows the sROI representation of cortical regional quantification and statistical data provided by NeuroQ of the transaxial slice immediately above it. For sROI's with metabolism falling in the lowest 5% of a normal distribution, hypometabolism is color-coded according to the two-dimensional scale shown at the top left

(horizontal axis, magnitude of hypometabolism; vertical axis, number of standard deviations below mean values in database of asymptomatic control subjects), ranging from blue (least hypometabolic) to red (most hypometabolic).

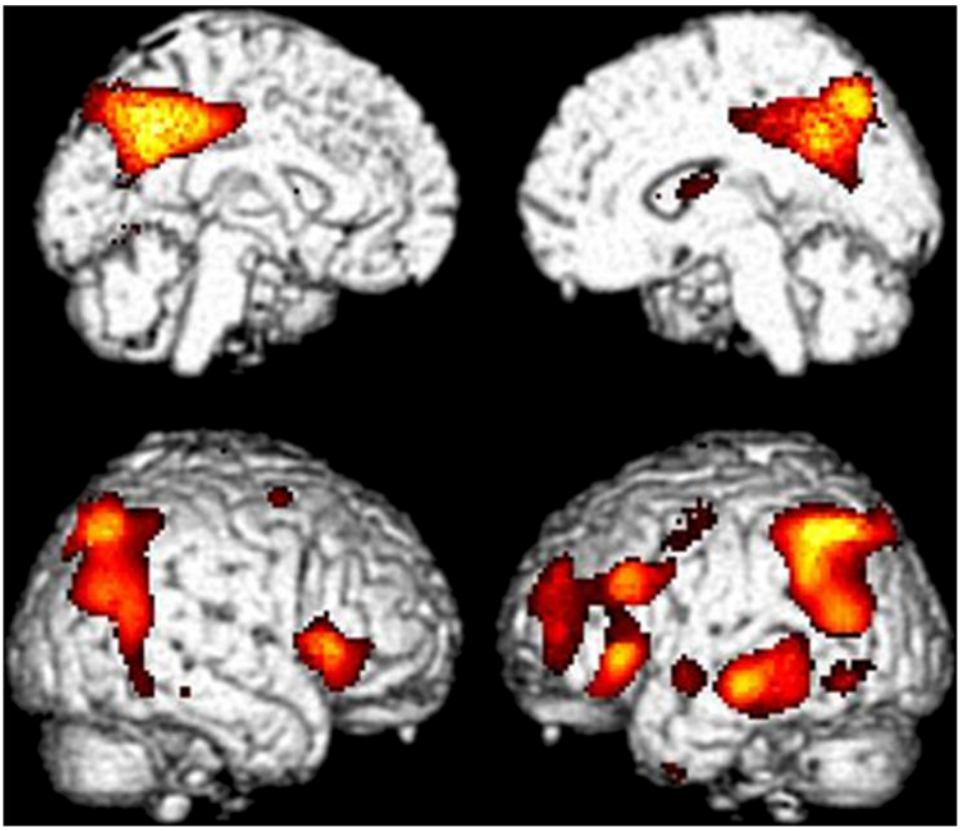

Figure 2.

Statistical Parametric Mapping of FDG-PET images comparing subjects in the High Frontal/ Parietal (HF/PA) FDDNP binding subgroups with Subjects in the Low Global (LG) FDDNP binding subgroup. The color scale highlights the location of all cortical voxels ($p < 0.01$) in which lower metabolism occurred in the HF/PA group than in the LG group., Hypometabolism in HF/PA relative to LG was found in the following regions: right perisylvian, with peak significance at 38,20,4; $t = 5.05$, $p < 0.0005$, $p_{voxelcorrected} = 0.03$; left mid-temporal gyrus with peak significance at −70, −28, −12; $t = 4.66$, $p < 0.0005$; left inferior parietal/ parietotemporal hypometabolism with peak significance at −56, −50,44; $t = 4.64$, $p < 0.0005$, $p_{clustercorrected} = 0.001$; bilateral posterior cingulate cortex (right greater than left), with peak significance at 6, −54,38; $t = 4.59$, $p < 0.0005$, largest cluster with 6992 contiguous voxels, $p_{clustercorrected} < 0.0005$; Left dorsolateral prefrontal cortex, with peak significance at −38,52,30, $t = 3.84$, $p < 0.0005$, $p_{clustercorrected} = 0.01$.

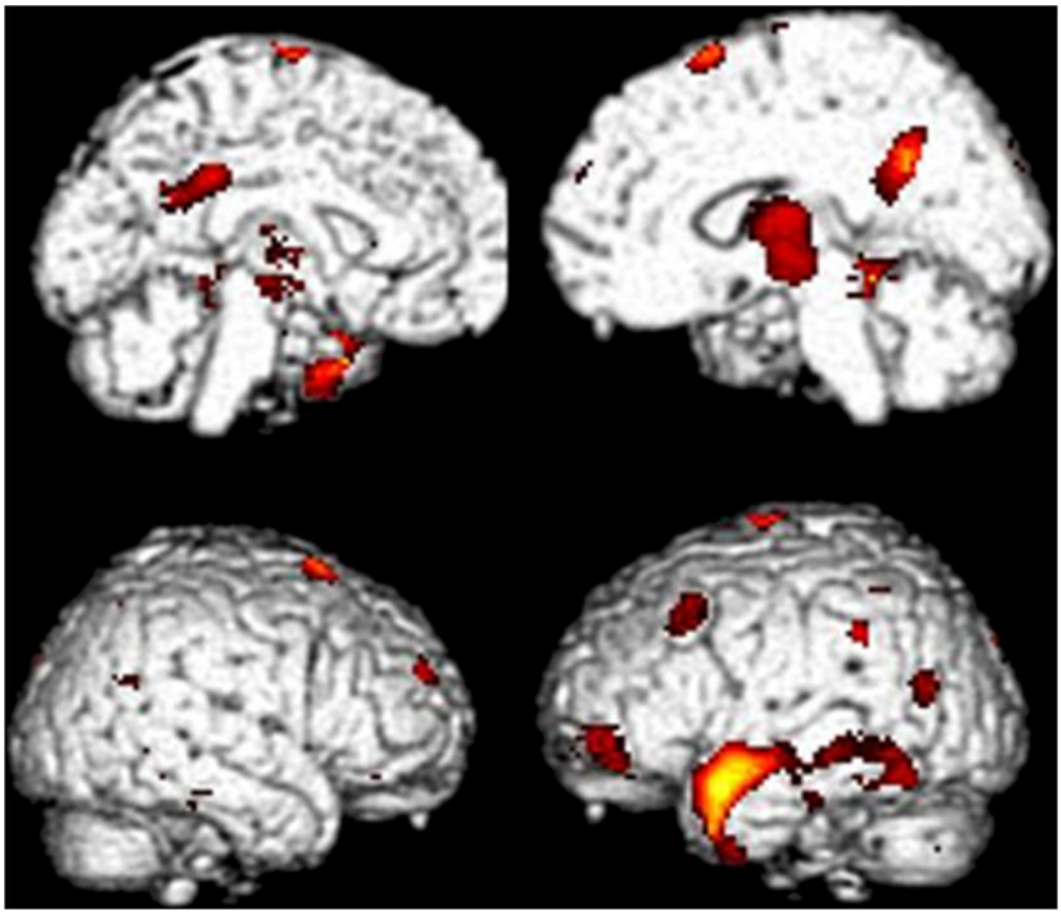

Figure 3.

The color scale highlights the location of all cortical voxels ($p < 0.01$) in which lower metabolism occurred in the HT/PC group than in the LG group. Hypometabolism in HT/PC relative to LG was found in the following regions: bilateral parahippocampal gyrus (left greater than right) with peak significance at −36, −34, −10; $t = 4.36$, $p < 0.0005$, largest cluster with $p_{clustercorrected} = 0.003$; left mid frontal –inferior frontal gyrus interface at Brodman's 10 with peak significance at −50,52, −2; $t = 3.99$, $p < 0.0005$; left anterior middle temporal gyrus with peak significance at −52,2, −16; $t = 3.61$, $p = 0.001$; bilateral posterior cingulate cortex with peak significance at −20, −52,26; $t = 3.56$, $p = 0.001$.

Table 1

Subject demographic variables

	Diagnostic Groups		
Characteristic	**MCI (N = 28)**	**Control (N = 26)**	**All Subjects (N = 54)**
Age — yr	68.1 ± 11.8	67.3 ± 11.7	68.2 ± 11.4
Education — yr	16.2 ± 2.9	17.7 ± 2.6	17.1 ± 3.0
Female sex — no. (%)*	16 (57)	9 (34)	25 (46)
AD family history—no (%)	12 (43)	13 (50)	25 (46)
APOE-4 carrier— no. (%)†	9 (36)	13 (50)	22 (43)
Mini Mental State Exam‡	27.6 ± 1.8	29.1 ± 1.3	28.2 ± 1.7
Estimated Verbal IQ§	110.3 ± 8.4	117.3 ± 6.1	113.6 ± 8.1
HRSD-21	1.9 ± 2.4	2.3 ± 2.4	2.2 ± 2.4

MCI = Mild Cognitive Impairment; AD = Alzheimer's disease; APOE-4 = Apolipoprotein Epsilon-4; HRSD = Hamilton Rating Scale for Depression 21-item version.

*$X^2(1) = 3.92$, $p = 0.05$;

†APOE-4 missing for 3 MCI subjects;

‡$t(53) = 4.4$, $p < 0.0001$.

§Intelligence Quotient estimated using adult reading tests (the Wechsler Test of Adult Reading, N = 8; or the National Adult Reading Test, N = 41); $t(47) = 3.32$, $p = .002$. N = 5 missing values,

Table 2

Diagnostic Group and Memory Domain Z Scores of the FDDNP Clusters.

	FDDNP Signal Clusters		
Diagnostic Group	**No. of subjects per cluster**		
	LG	**HF/PA**	**HT/PC**
Normal cognition	19	7	1
MCI	5	17	7
MCI-A	4	7	2
MCI-A+	1	10	5
Mean (SD) Domain Z Scores for Clusters*			
	LG	HF/PA	HT/PC
Memory†	.59 (.70)	−.33 (.81)	−.43 (.56)
Executive‡	.48 (.49)	−.42 (1.04)	−.28(1.02)

LG = Low Global; HF/PA = High frontal/parietal and medial temporal signal with intermediate signal in temporal and posterior cingulate; HT/PC = High lateral temporal/posterior cingulate. MCI-A = single domain amnestic mild cognitive impairment; MCI-A+ = multiple domain amnestic mild cognitive impairment.

*Lower (more negative) Z scores represent poorer performances.

†Memory Domain: [F(2,46) = 8.07, p = .001; LG vs HF/PA: t(46) = 3.82, p = .0004; LG vs HT/PC: t(46) = 2.39, p = .02];

‡Executive Domain [F(2,46) = 5.25, p = .01; LG vs HF/PA: t(46) = 3.24, p = .002]

Table 3

Number and Cognitive Status of Subjects in FDG-PET visual rating and FDDNP-PET Subgroups.

	FDDNP-PET Pattern		
Visual Rating of FDG-PET Pattern	**LG N = 23**	**HT/PC N = 7**	**HF/PA N = 24**
AD-like*	5 (3/1/1)	2 (0/1/1)	14 (1/5/8)
Non-AD-like*	18 (15/3/0)	5 (1/1/3)	10 (6/2/2)

PET = Positron Emission Tomography; FDG = 2-deoxy-2-[F-18]fluoro-D-glucose; FDDNP = 2-(1-{6-[(2-[F-18]fluoroethyl)(methyl) amino]-2-naphthyl} ethylidene)malononitrile; AD-like = Alzheimer's disease like FDG-PET pattern; LG = Low global FDDNP binding; HT/PC = high FDDNP binding in medial and lateral temporal and posterior cingulate regions; HF/PA = high FDDNP binding in frontal, parietal and medial temporal regions.

*Frequencies are for Total Subjects (Cognitively Normal/MCI-A/MCI-A+).